

DEVELOPMENT AND EVALUATION OF AN IMPROVED ALGORITHM FOR ESTIMATING THERMAL INTERNAL BOUNDARY LAYER HEIGHT¹

Ronald L. Petersen
Cermak Peterka Petersen, Inc.
1415 Blue Spruce Drive
Fort Collins, CO 80524

Summary

A meteorological condition that can produce high concentrations in coastal environments is referred to as shoreline fumigation. Past studies have shown that an important parameter for predicting accurate concentrations under this conditions is the height of the thermal internal boundary layer (TIBL) versus inland distance. While several analytical methods have been developed for estimating TIBL height, one method, referred to as the Weisman equation, has been shown to provide better estimates than several other methods when compared against field observations. The Weisman equation was developed based on the assumption of constant overwater temperature lapse rate, uniform overland wind profile, constant surface heat flux, and zero heat flux at the top of the TIBL. This paper presents a new equation for predicting the TIBL height which does not include these assumptions and which is based on sound scientific principles. The new equation was tested against a wind tunnel and field database of TIBL heights and the new equation agreed significantly better with observations (at the 95% confidence level) than the existing Weisman equation. Based on this study, the new TIBL algorithm should be inserted into an appropriate shoreline dispersion model so that the overall model performance with this algorithm can be evaluated against field and wind tunnel databases.

Introduction

A meteorological condition that can produce high concentrations in coastal environments is referred to as shoreline fumigation. The condition occurs when the air flows from the ocean (or other large water body) toward the land. At the land-sea interface, a new internal boundary layer begins to develop due to

¹ Submitted to the Journal of Wind Engineering and Industrial Aerodynamics for publication in April of 1999. Do not cite until published.

mechanical and thermal effects. When the land is much warmer than the water surface and the land surface roughness is not extreme, thermal effects will dominate and a thermal internal boundary layer (TIBL) begins to develop. The height of the TIBL versus downwind distance, x , has been shown to grow in proportion to $x^{1/2}$ ^{1,2}. Below the TIBL, the atmosphere is typically unstably stratified while above the TIBL, a stable temperature lapse rate is usually assumed. The fumigation condition occurs when a plume initially released into the stable flow above the TIBL, intersects the TIBL. At the point of intersection, the bottom portions of the plume are mixed toward the ground due to the turbulent eddies within the TIBL. As more and more of the plume enters the TIBL, more is mixed toward the ground which in turn can result in high ground level concentrations. Since this condition can persist for several hours, it is not a transient situation and without proper emission controls ambient air quality standards can be exceeded. Alternately, in situations where this is an infrequent condition, it may be more advisable to shut down plant operations until the condition passes.

SethRaman³ conducted an evaluation of six formulas for estimating TIBL height. The formulas evaluated were referred to as Weisman¹, Plate⁴, Van der Hoven⁵, Peters⁶, Raynor⁷, and Venkatram⁸. SethRaman³ found seven potential field databases that documented TIBL heights and concluded that two of the databases^{9, 10, 11} provided sufficient information for evaluating the TIBL formulas. These two databases provided twenty-nine hours of TIBL measurements and 203 TIBL height observations. The six TIBL formulas were statistically evaluated against the field databases with the conclusion that the Weisman¹ formulation predicted TIBL heights best. It should be noted that even though the Weisman¹ formulation produced the best agreement, the formula was developed on the basis of a uniform distribution of surface heat flux with inland distance, uniform wind and temperature profiles, and zero heat flux at the top of the TIBL.

SethuRaman³ also conducted an evaluation of the CRSTER Shoreline Fumigation Model (CSFM) and Misra¹² Shoreline Fumigation Model (MSFM) along with variations of the MSFM model. All models used the Weisman TIBL formulation. The MSFM and CSFM models were evaluated against the Nanticoke field database¹³. This database consisted on 13 test cases all of which met the criteria of daytime onshore flow and sufficient land-water temperature difference. The statistical evaluation of the

models showed that the MSFM model performed best. The results of the evaluation also showed that the TIBL formulation was the largest contributor to model prediction variation. As a result it was concluded that the TIBL formulation is the key to coastal dispersion modeling. It should also be noted that MSFM is also the basic model that the Environmental Protection Agency¹⁴ recommends for use when estimating concentrations under the shoreline fumigation situation.

Based on the above, it is clear that enhancements to the TIBL formula could significantly improve the predictive capability of the dispersion models presently in use for estimating concentrations for the shoreline fumigation situation. Hence, the purpose of this paper is to present a new TIBL formulation that accounts for the non-uniformity of the wind and temperature with height, the non-uniformity of the surface heat flux with inland distance, and a non-zero heat flux at the top of the TIBL. The new TIBL formulation was developed and tested based upon wind tunnel experiments¹⁵ conducted in an environmental wind tunnel like that described in Meroney². After the initial development and testing of the algorithm, it was then tested against a field data base of TIBL height measurements²⁰.

New And Existing TIBL Height Prediction Algorithms

As discussed above, several analytical methods have been developed for estimating TIBL height, and one method, referred to as the Weisman equation, has been shown to provide the best estimates when compared against field observations. The Weisman equation was developed based on the assumption of constant overwater temperature lapse rate, uniform overland wind profile, constant surface heat flux, and zero heat flux at the top of the TIBL and is provided below:

$$h_b = \sqrt{\frac{2H_{o,\infty}x}{\alpha C_p \rho U_L}} \quad (1)$$

where h_i is the height of thermal internal boundary layer (TIBL) at distance x (m); $H_{o,4}$ is the surface heat flux ($\rho C_p \overline{w'T_{0,\infty}}$) far inland (W/m^2); α is the overwater potential temperature vertical lapse rate (dT/dz); and U_L , the average wind speed within the TIBL (m/s).

A new TIBL equation (referred to as the Petersen algorithm) is developed here by going back to the basic conservation equations (mass, energy, and momentum). Based on these equations, Garatt¹⁵ presents the following partial differential equation (i.e., an integral equation) describing the growth of a convective boundary layer (i.e., TIBL height):

$$\frac{\partial h_t}{\partial x} = \frac{(1 + 2\beta)(H)_o}{\gamma C_p \rho h_t U_L} \quad (2)$$

where the new parameters are defined as follows

$$\beta = -\frac{\overline{w'T'_{h_t}}}{\overline{w'T'_o}} \quad (3)$$

$$H_o(x) = H_{o,\infty} \left(1 - \exp \left[-\frac{x}{a} \right] \right) = H_{o,\infty} f(x) \quad (4)$$

$$U_L = \frac{1}{h_t(x)} \int_0^{h_t(x)} U(z) dz \quad (5)$$

Now if we assume that $U(z)$ can be described by the wind power law equation, as follows,

$$U(z) = U_{ref} \left[\frac{h_t}{Z_{ref}} \right]^n \quad (6)$$

and Equation (6) is substituted into equation (5), the following equation results for estimating the mean velocity within the TIBL:

$$U_L = \frac{U_{ref}}{n+1} \left(\frac{h_t}{Z_{ref}} \right)^n \quad (7)$$

The reference wind speed (and associated height) should be from an inland station within the TIBL.

So that the lapse rate above the TIBL can be estimated as a function of downwind distance (or h_t),

the following power law relation for the temperature profile was assumed (note: temperature throughout this paper is potential temperature)

$$T(h_t) = (T_3 - T_0) \left(\frac{h_t}{Z_3} \right)^p + T_0 \quad (8)$$

The lapse rate as a function of height is then determined by differentiating with respect to z , as follows:

$$\frac{dT}{dz} = \gamma = (T_3 - T_0) p \frac{h_t^{p-1}}{Z_3^p} \quad (9)$$

When Equations 4, 7 and 9 are substituted into Equation 2 and the equation is integrated from the initial TIBL height ($h_{t,o}$) to the TIBL height, the following equation results:

$$h_t = \left[\frac{z_{ref}^n z_3^p (1 + 2\beta)(n+1)(n+p+1)g(x)H_{0,\infty}x}{p(T_3 - T_0)C_p \rho U_{ref}} + h_{t,0}^{n+p+1} \right]^{\frac{1}{n+p+1}} \quad (10)$$

where

$$g(x) = \left(1 - \frac{a}{x} + \frac{a}{x} \exp\left(-\frac{x}{a}\right) \right) \quad (11)$$

Equation (10) can be rewritten in the following form

$$h_t = \left[A'' g(x)x + h_{t,0}^{n+p+1} \right]^{\frac{1}{n+p+1}} \quad (12)$$

$$A'' = \left[\frac{z_{ref}^n z_3^p (1 + 2\beta)(n+1)(n+p+1)H_{0,\infty}}{p(T_3 - T_0)C_p \rho U_{ref}} \right] \quad (13)$$

where

When $\beta=0$, $n=0$, $p=1$, $h_{t,o}=0$ and $a=1E-8$ (a number that approaches zero), Equation 13

reduces to the standard Weisman equation. The improvement over the Weisman equation comes when representative values for these parameters are specified. With regard to β , Garratt says that the value varies between 0 and 1 and that the most common value found from past experiments is 0.2. This term β represents the ratio of heat flux at the top of the TIBL to that at the surface. Notice that the heat flux at the top of the TIBL is in the opposite direction (i.e., down) as that at the surface (when it is non-zero).

Databases for Evaluating TIBL Height Predictions

To evaluate the adequacy of the new TIBL equation, wind tunnel and field databases of observed TIBL heights were obtained. The following provides a descriptions of the databases.

Wind Tunnel TIBL Height Database

Wind tunnel simulation techniques similar to those described in Meroney² were used to develop a database of TIBL heights for a range of meteorological conditions. The limitations on wind tunnel and numerical modeling for simulating this condition are discussed in Avvissar¹⁶ and wind tunnel simulation methods are discussed by Cermak¹⁷ and Snyder¹⁸. All testing was conducted at a 1:400 model scale in the Colorado State University meteorological wind tunnel². The wind tunnel is shown schematically in Figures 1a and 1b. Figure 1b shows that 9.8 m of cooling plates were installed upwind of the land/sea interface. The plates were rippled and the simulated surface roughness was approximately 1 cm, slightly rougher than an ocean surface. Downwind of the land/sea interface, 12.2 m of 7.6 cm square roughness flaps were installed on top of the permanently installed heating plates. The roughness simulated a 50 cm land surface roughness length.

The boundary layer measurements and simulation techniques discussed in Petersen¹⁹ were used to develop a database of TIBL heights versus distance from the simulated shoreline along with appropriate meteorological parameters for use in calculating the TIBL height. The TIBL height was defined based on temperature profiles measured at six distances (100, 250, 400, 700, 1300 and 2500 m) downwind of the simulated shoreline. The TIBL height was taken to be the height where the temperature profile became isothermal. Figure 2 is provided as an example and shows the measured temperature profile versus inland

distance for one of the conditions simulated (i.e., Condition 3). Five different meteorological conditions were simulated and full scale parameters for each simulation are provided in Table 1. The observed TIBL heights are provided in Table 2. Since detailed boundary layer documentation was not obtained for Condition 1, some of the meteorological parameters in Table 1 (i.e., surface heat flux) were estimated based on wind and temperature profile measurements.

With regard to the common inputs for the Weisman or Petersen TIBL algorithms, the surface heat flux was measured in the wind tunnel at a full scale height of 4 m above ground level at each downwind distance. The far inland value was taken to be the average of the values measured at the last two downwind distances (i.e., 1300 and 2500 m). The overwater potential temperature lapse rate was calculated using the potential temperature at heights of 32 m (T_2) and 4 m (T_1) for the Weisman algorithm and 100 m (T_3) and 4 m (T_1) for the Petersen algorithm. The 32 m and 4 m heights are the approximate measurement heights for typical overwater buoy data. The reference wind speed, U_{ref} , was taken at a 100 m height at the far inland distance (i.e., $x = 2500$ m). This 100 m input can be obtained in the field from wind profiler data or data at any height can be used and scaled to 100 m using wind power law relations as described under the new method. The Petersen method actually estimates the average wind speed within the TIBL based on measurements at any height within the TIBL.

With regard to the inputs specific to the Petersen algorithm, the a constant in Equation 4 was found by minimizing the mean square error between wind tunnel observations of surface heat flux and Equation 4. The computed a value was used as input for Conditions 2 through 5. Since H_o was not measured for Condition 1, the average value of 654 for a from the other four conditions was used for Condition 1. Table 1 also shows that the best-fit a values for each condition varied from 479 to 811.

The wind power-law exponent, n , would most likely vary with downwind distance and will not generally be available from routine field observations. Therefore, the value associated with a particular overland stability and roughness should be specified for routine use in an appropriate shoreline dispersion model. For this database, a power-law exponent was determined for each condition using the measured profile at the far inland distance. The power-law exponent was observed to vary between 0.059 and

0.160, which is reasonable for an unstable atmospheric boundary layer. The measured values were used for each condition.

The temperature power-law exponent was initially estimated by fitting Equation 8 to the approach-temperature profile for each condition. Some of the profiles were irregularly shaped and had power-law fits which did not look reasonable. However, the best-fit values were used as inputs for evaluating the new TIBL equation.

The initial TIBL height was taken to be the height of the roughness elements over land. This is a reasonable assumption, since the initial boundary layer would be some function of the roughness height; however, more work needs to be carried out in this area. Some sensitivity tests were carried out which showed that the lowest root-mean-square error between predicted and observed TIBL heights was obtained using approximately the roughness height value. The value for β was taken to be zero based the wind tunnel observations.

Field TIBL Height Database

An extensive field measurement program was conducted to study coastal fumigation of a plume from the coal-fired power plant at Nanticoke, Ontario in June of 1978¹³. The power plant is located on the north shore of Lake Erie near the town of Nanticoke. During the course of the field testing, observations of the structure of the internal boundary layer were made on eight days²⁰. Two of the days, June 1 and June 6 were judged to have the most complete set of observations regarding the growth of the TIBL. This database was selected for testing the new algorithms for the following reasons: 1) this database was also used to evaluate the Weisman equation^{3,22}; and 2) sufficient information was obtained in field so that estimates could be obtained using the Petersen algorithm with some of the enhancements.

The field measurement results and necessary meteorological data for June 1 and 6, 1978 are summarized in Tables 3 and 4²⁰. Two additional parameters are reported in the tables, dT/dz and p , that were not reported in Kerman²⁰. These parameters are needed for input into the Weisman and Petersen

TIBL algorithms and were computed as follows. First, N_e is defined as follows:

$$N_e = \frac{1}{h^2} \int_0^h N^2 dz^2 \quad (14)$$

where $N^2 = g T^{-1} dT/dz$. Taking the g/T out of both sides of the equation results in the following:

$$\frac{dT}{dz_{avg}} = \frac{1}{h^2} \int_0^h \frac{dT}{dz} dz^2 \quad (15)$$

Now if equation 9 is substituted into the right side of the above equation and the integration is carried out, the following equation results:

$$\frac{dT}{dz_{avg}} = \frac{2(T_3 - T_0)}{z_3^p} \frac{p}{p+1} h^{p-1} \quad (16)$$

The average dT/dz was computed at each measurement height in Tables 3 and 4 and “p” was determined by minimizing the error between left and right side of the above equation.

With regard to the common inputs for the Weisman or Petersen TIBL algorithms, the surface heat flux, overwater potential temperature lapse rate, average wind speed, U_{avg} are listed in Tables 3 and 4. With regard to the inputs specific to the Petersen algorithm, the a constant was set to zero since no specific data on the variation of heat flux with inland distance was available. Since the average wind speed within the TIBL was provided, the wind power-law exponent n is equal to zero. The temperature power-law exponent, p , was estimated as discussed above and is provided in Tables 3 and 4. The initial TIBL height was taken to be the zero as was the value for β . Other constants are summarized in Tables 3 and 4.

Evaluation of TIBL Algorithms

TIBL height versus downwind distance was computed for each of the databases described above using the inputs in Tables 1-4 and the equations discussed previously. To provide a qualitative assessment

of the Petersen and Weisman methods, graphs were generated showing the computed and observed TIBL heights versus downwind distance for each database. The plots are shown in Figures 3-5. Figure 3 shows that the Petersen method agrees best with wind tunnel observations for all meteorological conditions simulated. The Weisman method tends to underestimate the TIBL height. Figures 4 and 5 show that the Petersen and Weisman methods give similar estimates for many cases but the Petersen method tends to give overall better agreement with observations. Both methods tend to under predict the TIBL height but the Weisman method under predicts by a greater margin.

Figures 6a through 6c show the ratio of observed to predicted TIBL height versus downwind distance for each database. The figures confirm the previous conclusion that the Weisman method tends to overpredict by a greater margin and the Petersen method agrees better with observations at all downwind distances.

For a more quantitative assessment, a statistical evaluation was conducted using the BOOT program²³ to assess which method agrees best with observations (Petersen or Weisman). Three statistical quantities were calculated, the fractional bias (*FB*), the normalized mean square error (*NMSE*) and the fraction of estimates within a factor of two of observations (*Fac2*). The *FB* and *NMSE* are defined as follows:

$$FB = \frac{\overline{h_{t,ob}} - \overline{h_{t,p}}}{0.5(\overline{h_{t,ob}} + \overline{h_{t,p}})}, \quad (17)$$

$$NMSE = \frac{\overline{(h_{t,ob} - h_{t,p})^2}}{\overline{h_{t,p}} \overline{h_{t,ob}}} \quad (18)$$

where $h_{t,ob}$ is the observed TIBL height from the wind tunnel or field and $h_{t,p}$ is the predicted TIBL height obtained using Petersen or Weisman. Perfect agreement between two methods is indicated when $FB = NMSE = 0$. The definition of *Fac2* is self evident.

The FB , $NMSE$ and $Fac2$ were computed for each database (i.e., wind tunnel, June 1-field and June 6-field) and for all databases combined. Table 5 provides a listing of the FB , $NMSE$ and $Fac2$ for each method for the different data groupings. Table 5 shows that FB and $NMSE$ are consistently lower for the Petersen method and the FB considering all databases is 0.23 (an under prediction). The corresponding FB for the Weisman method and all databases is 0.64. The respective $NMSE$ for Petersen and Weisman for all databases is 0.24 and 0.89. With regard to the number of estimates within a factor of two of observations, 91% of the Petersen estimates meet the criteria while only 56% of the Weisman estimates.

Another type analysis was conducted to assess whether the FB and $NMSE$ are significantly different for the Petersen and Weisman methods. To make this assessment, the differences in fractional bias (FB) and normalized mean square error ($NMSE$) between the Petersen and Weisman methods were computed using the BOOT program²³. Figure 7 shows the resulting differences in fractional bias (FB) and normalized mean square error ($NMSE$) for the two methods compared to one another using the complete data set (i.e., wind tunnel, June 1- field and June 6 - field). Similar methods in the figures will have the 95% confidence interval overlap the zero value for $D(FB)$, and $D(NMSE)$ will be close to zero. Figure 7 show that the FB differences between the Petersen and Weisman methods are significantly different at the 95% confidence for each database. The differences in $NMSE$ are also approximately zero for the June 1 database but significantly different from zero for the other databases. Hence, the Petersen method provides statistically significant different estimates and estimates that agree better with observations.

Conclusions

The above analysis has shown that the Petersen algorithm (Equation 12) provides significantly better estimates (at the 95% confidence level) of TIBL heights as observed in the wind tunnel and field than the Weisman equation. The Petersen algorithm has the following features: 1) with $\beta = 0$, $n = 0$, $p=1$, $h_{t,o} = 0$ and $a = 0$, the equation reduces to the Weisman equation; 2) it is based on sound scientific principles with fewer limiting assumption than Weisman; 3) it accounts for the variation of the mean wind speed with inland distance within the TIBL; 4) it accounts for the variation of surface heat flux with inland distance; and

5) it accounts for the variation of temperature lapse rate with height.

Since earlier work^{3,22} showed that the TIBL height was a critical parameter affecting dispersion model performance, it is anticipated that the new algorithm, when included in a shoreline dispersion model, will ultimately help provide better concentration estimates for that situation. While other algorithms have been suggested in the literature^{24,25,26,27}, the Weisman algorithm is presently used in an EPA shoreline dispersion model¹⁴ and other investigators have used Weisman or equations that are very similar. The new equation should be inserted into a shoreline dispersion model so that the overall performance of the model with this algorithm can be evaluated using wind tunnel data and available field databases³.

Further testing of the new TIBL equation against more detailed field observations is recommended for the future. Measurement of surface heat flux versus inland distance and the inland wind profile shape may further improve the agreement with field observations. Several aspects of the wind tunnel observation also need further evaluation. First, the observed variation of heat flux with height, and second the observed variation of surface heat flux with inland distance. It is also suggested that the RAMS model¹⁶ (or equivalent) be used to simulate the wind tunnel experiments. These simulations can be used to develop a better understanding of the wind tunnel results and to generate additional data sets for testing the new TIBL algorithm. Other areas that need investigation include, the method for specifying the power law exponents in the field, the method for obtaining overwater temperatures, and a method for specifying β for different boundary layers.

Acknowledgments

The author would like to acknowledge the contributions of several individuals and organizations who contributed to this research effort. First, to Dr. Richard Dunk at Jersey Central Power and Light for financial and technical support; second, to Mr. Brad Cochran and Mr. Steve Mike of CPP for their assistance in collecting and analyzing the wind tunnel data; then to Drs. Robert E. Meroney and David E. Neff from Colorado State University for coordinating the use of the CSU meteorological wind tunnel and instrumentation.

References

- 1) B. Weisman, Response to: On the Criteria for the Occurrence of Fumigation Inland from a Large Lake. *Atmospheric Environment*, 12, (1976) 172–173.
- 2) R.N. Meroney, J.E. Cermak, and B.T. Yang, Modeling of atmospheric transport and fumigation at shoreline sites, *Boundary Layer Meteorology*, 9, (1975) 69-90.
- 3) S. SethuRaman, Analysis and evaluation of statistical coastal fumigation models, U.S. EPA, Research Triangle Park, NC, EPA-450/4-87-002, 1987.
- 4) E. J. Plate, Aerodynamic characteristics of atmospheric boundary layers, United States Atomic Energy Commission, 1971.
- 5) I. Van der Hoven, Atmospheric transport and diffusion at coastal sites, *Nuclear Safety*, 8, (1967) 490-499.
- 6) L.K. Peters, On the criteria for the occurrence of fumigation inland from a large lake, *Atmospheric Environment*, 9, (1975) 809–816.
- 7) G.S. Raynor, P. Michael, R. M. Brown, and S. SethuRaman, Studies of atmospheric diffusion from a near shore oceanic site”, *J. Appl. Meteor.*, 14, (1975) 1080-1094.
- 8) A. Venkatram, A model of internal boundary-layer development, *Boundary Layer Meteorology*, 11, (1977) 419-437.
- 9) G.S. Raynor, S. SethuRaman and R. M. Brown, Formation and characterization of coastal internal boundary layers during onshore flows, *Boundary Layer Meteorology*, 16,(1979) 487-514.
- 10) M.S. Gamo, S. Yamamoto, O. Yokoyama and F. Yashikado, Structure of the free convective internal boundary layer above the coastal area, *J. Meteor. Soc. Japan*, 61, (1983) 110-124.
- 11) M.S. Gamo, Airborne measurements of the free convective internal boundary layer during the sea breeze, *J. Meteor. Soc. Japan*, 60, (1982) 1284-1298.
- 12) P.K. Misra, Dispersion from tall stacks into a shoreline environment, *Atmospheric Environment*, 14, (1980) 396-400.
- 13) R.V. Portelli, The Nanticoke shoreline diffusion experiment, June 1978-I. Experimental design and program overview, *Atmospheric Environment*, 16, No.3, (1982) 413-421.
- 14) EPA, *User's Guide to SDM—A Shoreline Dispersion Model*. U.S. Environmental Protection Agency, Office of Air Quality Planning and Standards, EPA-450/88-017, 1988.
- 15) J.R. Garratt, *The Atmospheric Boundary Layer*, Cambridge University Press, Great Britain, 1992.

- 16) R. Avissar, M.D. Moran, G. Wu, R.N. Meroney, and R. A. Pielke, Operating ranges of mesoscale numerical models and meteorological wind tunnels for the simulation of sea and land breezes,” *Boundary Layer Meteorology*, 50, (1990) 227-275.
- 17) J.E. Cermak, Applications of fluid mechanics to wind engineering - A Freeman Scholar Lecture, *Journal Fluids Engineering*, 97, (1975) 9-38.
- 18) W.H. Snyder, Guideline for Fluid Modeling of Atmospheric Diffusion, USEPA, Environmental Sciences Research Laboratory, Office of Research and Development, Research Triangle Park, NC, Report No. EPA600/8-81-009, 1981.
- 19) R.L. Petersen, B.C. Cochran, and A. Womble, Evaluation of TIBL Growth, Plume Rise and Dispersion under the Shoreline Fumigation Condition - A Wind Tunnel and Analytical Evaluation,” Cermak Peterka Petersen, Inc., 1415 Blue Spruce Drive, Fort Collins, CO, Project 1244, Sponsored by New Jersey Power & Light, January, 1997.
- 20) B.R. Kerman, R.E. Mickle, R.V. Portelli, N.B. Trivett, and P.K. Misra, The Nanticoke shoreline diffusion experiment, June 1978 - II. Internal boundary layer structure, *Atmospheric Environment*, 16, No.3, (1982) 423-437.
- 21) H.A. Panofsky and J.A. Dutton, *Atmospheric Turbulence: Models and Methods for Engineering Applications*. John Wiley & Sons, 1984.
- 22) M. Stunder and S. SethuRaman, A comparative evaluation of the coastal internal boundary-layer height equations, *Boundary -Layer Meteorology*, 32, (1985) 177-204.
- 23) American Petroleum Institute, Hazard Response Modeling Uncertainty (A Quantitative Method), Volume I, User's Guide for Software for Evaluating Hazardous Gas Dispersion Models, American Petroleum Institute, Publication No. 4545, Washington, DC, 1992.
- 24) S.R. Hanna, L.L. Schulman, R.J. Paine, and J.E. Pleim, Development and evaluation of the offshore and coastal dispersion model,” *JAPCA*, 35, (1985) 1039-1047.
- 25) M.F. Hibberd and A.K. Luhar, A laboratory study and improved PDF model of fumigation into a growing convective boundary layer,” *Atmospheric Environment*, 30, No. 21, (1996) 3633-3649.
- 26) A.K. Luhar and B. L. Sawford, An Examination of Existing Shoreline Fumigation Models and Formulation of an Improved Model, *Atmospheric Environment*, 30, No. 4, (1996) 609-620.
- 27) H. Jin and S. Raman, Dispersion of an elevated release in a coastal region, *Journal of Applied Meteorology*, 35, (1996) 1611-1624.

Figure 1a — Overall plan view of meteorological wind tunnel used to simulate the shoreline fumigation condition.

Figure 1b — Close up plan view of wind tunnel setup.

Figure 2 — Plot of temperature versus height observed in the wind tunnel at various downwind distances for Condition 3. The figure shows the growth of the TIBL with inland distance.

Figure 3 — Plot of observed and computed TIBL heights versus inland distance: a) Condition 1; b) Condition 2; c) Condition 3; d) Condition 4; and e) Condition 5.

Figure 4 — Plot of observed and computed TIBL heights versus inland distance - June 1 field database.

Figure 5 – Plot of observed to computed TIBL heights versus inland distance – June 6 field database.

Figure 6 – Ratio of observed to predicted TIBL heights versus downwind distance: a) wind tunnel database; b) June field1 database; c) June 6 field database.

Figure 8 – Differences in NMSE and FB for the two TIBL estimation methods.

APPENDIX A

Wind Tunnel Simulation Methods

Avissar¹⁶ presents a good summary of the of the limitations and the operating ranges for wind tunnel modeling of the sea and land breezes. Various references ^{16, 17, 18,} discuss the principles and limitations behind wind tunnel simulations in more detail. Based on these references, the criteria that were used to set up the wind tunnel simulations are as follows:

- C *geometric similarity* -- all physical lengths in the vertical and horizontal directions were reduced by a single scale ratio (1:400 for this study);
- C *matching approach maritime stability* -- this matching was achieved by setting the bulk over water Richardson number, Ri_{bulk} equal in model and full scale, where

$$Ri_{bulk} = \frac{gz_2(T_2 - T_1)_{water}}{(T_2 U_2^2)_{water}} \quad (\text{A.1})$$

and g is gravitational acceleration, T_2 and T_1 are potential temperatures at heights z_2 and z_1 , and U_2 is the wind speed at height z_2 ;

- C *matching approach maritime and land surface roughness values* -- the surface roughness length for the water surface $z_{o-water}$ and land z_{o-land} was set equal to an appropriate value as verified by analysis of the logarithmic wind profile under neutral conditions;
- C *equality of land/sea surface heating* -- the relative heating between the land and sea was modeled by matching of the ‘heating ratio’, HR , defined by:

$$HR = \frac{T_{1,land} - T_{1,water}}{(T_2 - T_1)_{water}} \quad (\text{A.2})$$

where $T_{1,land}$ is a near surface air temperature over the land. For comparing heating ratios, the measurement locations must be at geometrically similar locations. The overland temperature measurement location should be an appreciable distance inland to avoid variations with inland distance;

- C *sufficiently large Reynolds number* -- the tunnel wind speed should be sufficiently large so that the results are independent of Reynold number.
- C *similar dimensionless velocity, temperature and turbulence profiles*. Similar profile shapes are established by developing a natural boundary layer in the wind tunnel. The adequacy of the profile shapes is normally judged by comparison with log-linear profiles, as summarized below for a stable boundary layer.

$$U(z) = \frac{U_*}{k} \left(\ln \frac{z}{z_o} + 5 \frac{z}{L} \right) \quad (\text{A.3})$$

$$T(z) = \frac{T_*}{k} \left(\ln \frac{z}{z_o} + 5 \frac{z}{L} \right) + T_0 \quad (\text{A.4})$$

Equality of approach Richardson number and heating ratio described above forms the basis for converting model measurements to full scale quantities. These two quantities are known from model measurements. To determine full scale quantities (used for input to the TIBL algorithm) from model measurements, Equations 19 and 20 are used to define velocity and temperature difference scaling factors. A full land-sea temperature difference is first specified which defines the temperature difference scaling. It should be noted that the study results will be identical no matter what value is assumed here. In this study, the land-sea temperature difference was set to 4 degrees Kelvin for all conditions. Once the land-sea

temperature difference is set, the vertical temperature difference and the wind speed U_2 are established in full scale. The ratio of $U_{2\text{-full scale}}$ to $U_{2\text{-model}}$ becomes known since $U_{2\text{-model}}$ is measured. This velocity ratio can be applied to any other measurement point in the simulated domain due to dynamic similitude. This velocity ratio also applies to fluctuating velocities and quantities such as u_* , which is derived from fluctuating velocity components.

The full scale heat flux was determined from measurements of model quantities of u_* and heat flux through the following procedure. The model quantities u_* (friction velocity) and T_* (fluctuating temperature scale) were measured and are defined by:

$$u_* = \sqrt{-\overline{u'w'}} \quad (\text{A.5})$$

and

$$T_* = \frac{-\overline{w'T'}}{U_*} \quad (\text{A.6})$$

where u' , w' , and T' are fluctuations of longitudinal velocity, vertical velocity, and temperature. These measurements allow the Monin-Obukhov length scale, L_{m-o} in the model to be computed directly from the relation:

$$L_{m-o} = \frac{u_*^2 T}{T_* k g} \quad (\text{A.7})$$

Since this quantity has units of length, the full scale Monin-Obukhov scale can be computed by multiplying by the length scale ratio (1:400). Equating the dimensionless Monin-Obukhov length scale in model and full scale does not represent a unique additional scaling criteria since it relates a velocity scale to a vertical temperature difference scale just as the bulk Richardson number does. The Monin-Obukhov length scale is in terms of fluctuations while the bulk Richardson number is in terms of mean quantities; both relate to atmospheric stability and are dependent on each other. The full-scale values of u_* and L_{m-o} lead to the full scale value of T_* using a rearranged Equation 25. Sensible heat flux, H , is defined by:

$$H = \rho C_p \overline{w'T'} \quad (\text{A.8})$$

where ρ is atmospheric density and C_p is heat capacity of air (1006 J/kg/K). The full scale heat flux is computed using Equations 24 and 26 and full scale values of T_* and u_* .

TIBL and boundary layer growth was documented by measuring vertical profiles of temperature, wind speed, turbulence intensity (u' and w'), turbulent shear stress ($u'w'$), and turbulent vertical heat flux ($w't'$). Four meteorological conditions were established which were fully documented with detailed profile measurements. For each condition, one profile was collected over the water and five profiles were measured at various inland distances. The velocities were measured with hot wire anemometry with a two-dimensional X-wire configuration. Temperatures were measured with a sensitive thermocouple located within 5 mm of the X wire. The temperatures were also used to adjust the hot wire measurements for temperature variations. During profile measurements, tunnel wind speed and air temperatures at three locations were monitored.

From the land profile measurements, the TIBL heights were estimated by three methods: the height of the minimum temperature, the height at which turbulence intensity equals the approach condition, and the height at which vertical heat flux changes from positive to negative. The different methods produced somewhat similar results but the height of minimum temperature method was selected for use in evaluating the new TIBL algorithm. This method was selected because it is most likely the method that would also be used in the field.

Table 1
Full Scale Meteorological Parameters Simulated For Wind Tunnel Tests

Condition	1	2	3	4	5
Meteorological Parameters					
T ₃ , water (K)	300.39	300.43	301.59	300.57	300.84
T ₂ , water (K)	300.20	300.32	301.15	300.29	300.68
T ₁ , water (K)	300.00	300.00	300.00	300.00	300.00
T _{1b} , water (K)	299.56	299.54	298.84	299.42	298.76
T ₀ , land (K)	303.56	303.54	302.84	303.42	302.76
U ₃ , water	3.90	5.16	7.61	7.49	7.56
U ₂ , water	2.85	4.46	5.99	6.44	5.28
U ₁ , water	1.69	2.73	3.20	3.74	2.81
U _{ref} , land	3.99	6.30	7.37	7.74	8.49
Z ₃ (m)	100	100	100	100	100
Z ₂ (m)	32	32	32	32	32
Z ₁ (m)	8	4	4	4	4
Z _{ref} (m)	100	100	100	100	100
n _{land, water}	0.219	0.163	0.230	0.191	0.141
n _{vel, water}	0.274	0.180	0.247	0.203	0.311
n _{vel, land}	0.160	0.059	0.137	0.107	0.123
Sfc Heat Flx, land (W/m ²)	241.2	383.2	256.3	388.1	348.9
Sfc Heat Flx, water (W/m ²)	-2.20	-4.32	-18.06	-12.76	-3.55
a - Heat Flux Factor	654	582	811	479	745
L, land (m)	-54.2	-67.3	-204.9	-141.3	-144.3
L, water (m)	73.6	189.1	126.2	252.0	163.1
U _a , land (m/s)	0.510	0.663	0.839	0.852	0.828
U _a , water (m/s)	0.124	0.210	0.295	0.331	0.187
Z ₀ , land (m)	0.957	0.649	1.385	1.167	0.874
Z ₀ , water (m)	0.040	0.024	0.046	0.041	0.001

Table 2
Summary of TIBL Heights Observed in Wind Tunnel

Condition	x(m)	h_t (m)
1	250	80
	400	100
	700	160
	1300	220
2	100	24
	250	80
	400	120
	700	160
	1300	240
	2500	280
3	100	16
	250	28
	400	50
	700	80
	1300	160
	2500	280
4	100	32
	250	40
	400	70
	700	100
	1300	140
	2500	280
5	100	16
	250	32
	400	60
	700	100
	1300	140
	2500	200

Table 3

June 1, 1978 Field measurements documenting TIBL

L.S.T.	x (m)	h _t (m)	N _e (s-1)	dT/dz (K/m)	H _{0,inf} (W m-2)	U _{avg} (m/s)	Z _{ref} , Z ₃ (m)	p (-)	(T ₃ -T ₀) (K)
1100	2500	200	0.013	0.0050	184	3.8	200	1.47	1.0051
	5300	375	0.0175	0.0091					
	6000	400	0.017	0.0086					
	6700	420	0.0175	0.0091					
	8900	500	0.0164	0.0080					
1200	2100	175	0.0152	0.0069	234	4.8	175	0.92	1.2023
	4100	275	0.0148	0.0065					
	5500	325	0.0144	0.0062					
	6500	350	0.0139	0.0057					
	9000	450	0.0145	0.0063					
1300	1500	150	0.0212	0.0134	265	5	150	0.75	2.0046
	3600	250	0.018	0.0096					
	5600	350	0.0176	0.0092					
	8000	325	0.0177	0.0093					
	8800	375	0.017	0.0086					
1400	1400	125	0.0233	0.0163	265	5.1	125	0.80	2.0317
	3500	200	0.0233	0.0163					
	5300	275	0.0192	0.0110					
	7100	325	0.0188	0.0106					
	10500	425	0.0187	0.0105					
1500	1500	125	0.0233	0.0163	224	5	125	1.05	2.0386
	3400	200	0.026	0.0203					
	5500	250	0.0249	0.0186					
	9000	275	0.0238	0.0170					
	12500	300	0.0223	0.0149					
1600	1500	75	0.038	0.0434	177	5	75	0.71	3.2534
	3400	150	0.0355	0.0379					
	5500	230	0.0287	0.0247					
	6700	280	0.0255	0.0195					
	8900	300	0.0247	0.0183					
1700	1500	100	0.0427	0.0548	117	5	100	0.57	5.4773
	3300	175	0.0335	0.0337					
	5400	225	0.0285	0.0244					
	6900	250	0.027	0.0219					
	12800	275	0.0253	0.0192					

Note: $n=0$, $C_p = 1000 \text{ J/Kg/K}$; $\rho = 1.21 \text{ kg/m}^3$ for all cases

Table 4

June 6, 1978 Field measurements documenting TIBL

L.S.T.	x (m)	h_t (m)	N_e (s-1)	dT/dz (K/m)	$H_{0,inf}$ (W m-2)	U_{ref} (m/s)	Z_{ref}, Z_3 (m)	p (-)	(T_3-T_0) (K)
900	1800	175	0.0174	0.0089	106	5.5	175	0.93	1.5647
	6000	300	0.0164	0.0079					
	9000	320	0.0178	0.0094					
	12500	350	0.017	0.0085					
	18000	425	0.0154	0.0070					
1000	6000	300	0.019	0.0107	172	6.3	300	0.69	3.1983
	9000	360	0.0174	0.0089					
	12500	350	0.0175	0.0090					
	18000	525	0.0154	0.0070					
	25000	650	0.0124	0.0045					
1100	1800	200	0.0209	0.0129	246	6.5	200	0.74	2.5799
	6000	325	0.0199	0.0117					
	18000	500	0.016	0.0076					
	25000	625	0.0151	0.0067					
1200	1800	200	0.0219	0.0142	284	6	200	0.67	2.8425
	6000	325	0.0188	0.0105					
	12500	375	0.017	0.0086					
	18000	550	0.0147	0.0064					
1300	1800	150	0.0222	0.0146	330	6	150	0.82	2.1832
	6000	200	0.0221	0.0144					
	9000	320	0.0178	0.0094					
1400	1800	125	0.0344	0.0349	298	6.5	125	0.44	4.3683
	6000	200	0.0246	0.0179					
	9000	240	0.0198	0.0116					
	9500	250	0.0201	0.0119					
	13000	300	0.0164	0.0079					
1500	1800	125	0.0243	0.0174	275	6.5	125	0.51	2.1798
	6000	400	0.013	0.0050					
	13000	800	0.01	0.0030					
	18000	800	0.01	0.0030					
1600	1800	75	0.0258	0.0197	255	7	75	0.54	1.4743
	6000	500	0.0092	0.0025					
	18000	1150	0.0064	0.0012					
1700	1800	100	0.0184	0.0100	160	5.8	100	0.55	0.9998
	6000	400	0.01	0.0030					
	9500	550	0.0093	0.0026					
	18000	650	0.0085	0.0021					

Note: $n=0$, $C_p = 1000 \text{ J/Kg/K}$; $\rho = 1.21 \text{ kg/m}^3$ for all cases

Table 5
Summary of Statistical Analysis

FRACTIONAL BIAS (A positive value means method under predicts)

Database	TIBL Estimation Methods	
	Petersen	Weisman
Wind Tunnel	-0.06	0.97
Nanticoke - June 1	0.27	0.45
Nanticoke - June 6	0.28	0.69
All	0.23	0.64

NORMALIZED MEAN SQUARE ERROR

Database	Petersen	Weisman
Wind Tunnel	0.42	2.05
Nanticoke - June 1	0.11	0.27
Nanticoke - June 6	0.24	0.98
All	0.24	0.89

FRACTION WITHIN A FACTOR OF TWO

Database	Petersen	Weisman
Wind Tunnel	0.89	0.29
Nanticoke - June 1	0.86	0.74
Nanticoke - June 6	0.97	0.61
All	0.91	0.56

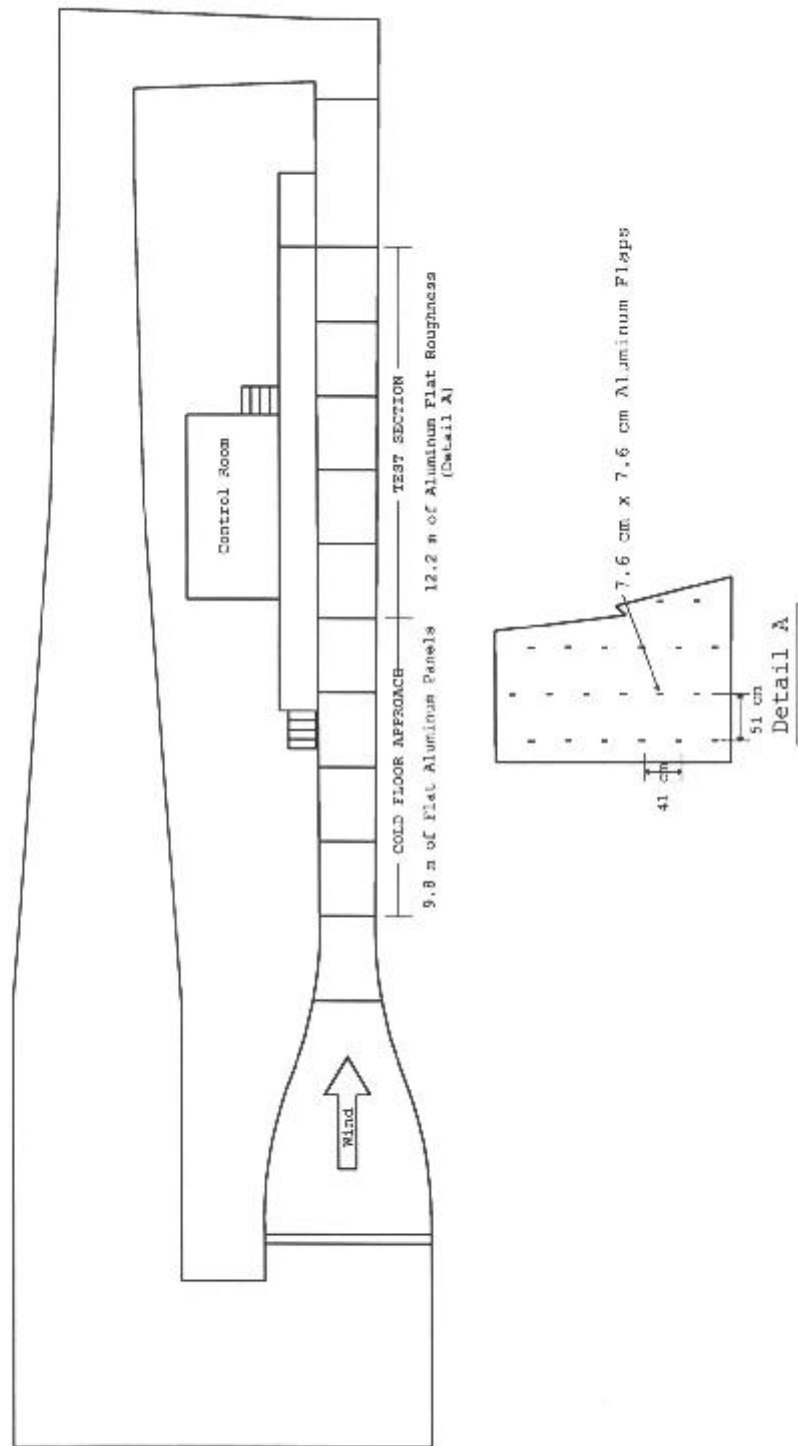


Figure 1a — Overall plan view of meteorological wind tunnel used to simulate the shoreline fumigation condition

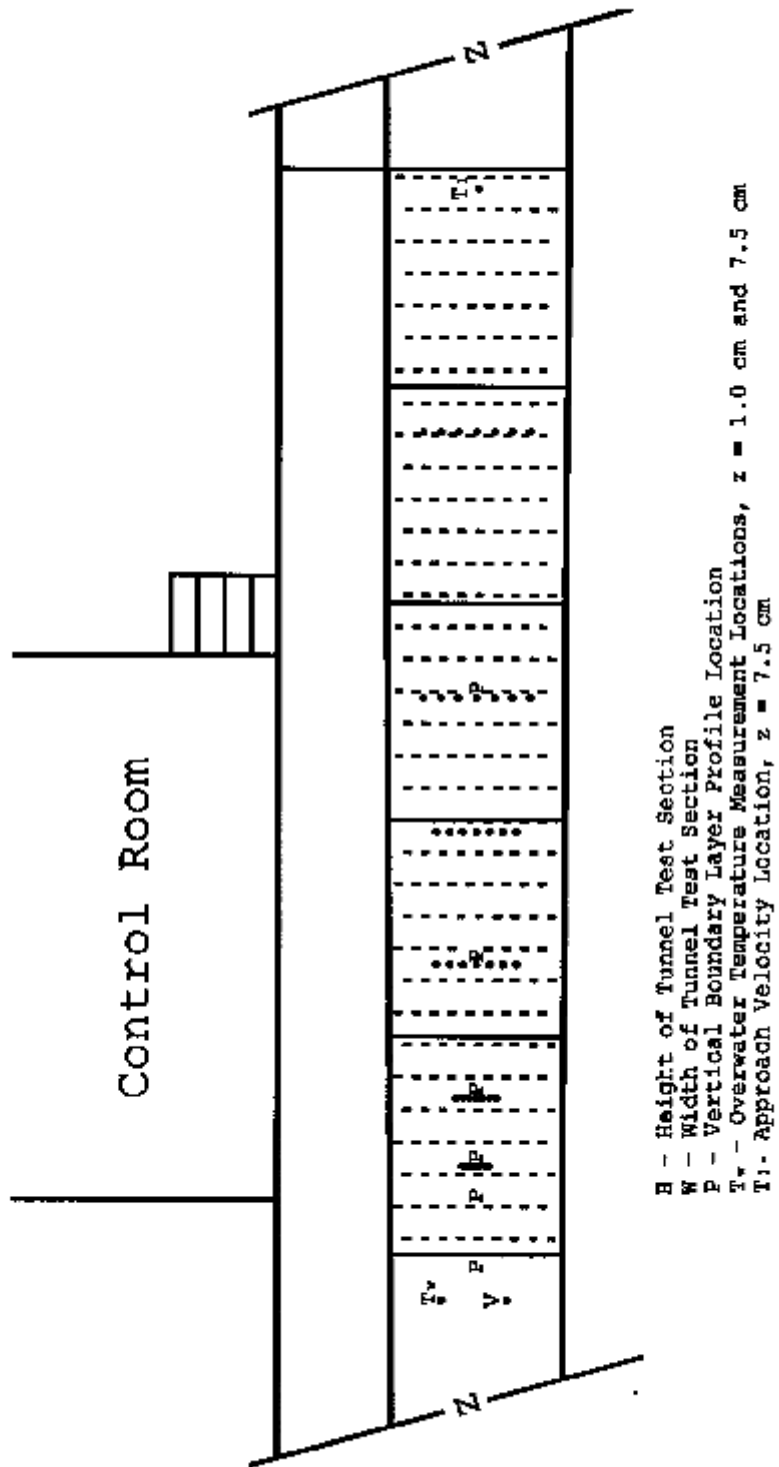


Figure 1b — Close up plan view of wind tunnel setup

Vertical Temperature Profiles

Condition 3 (July)

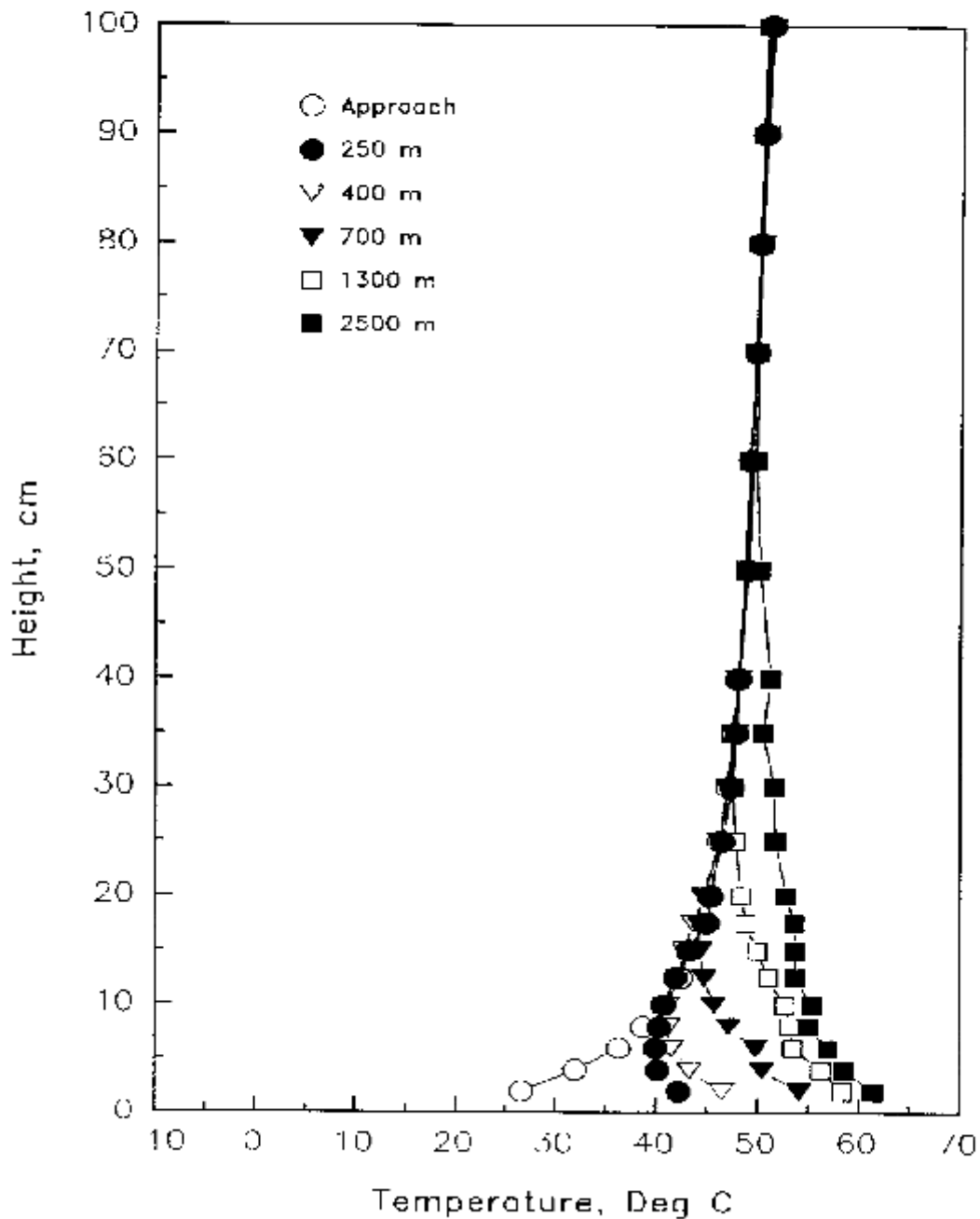


Figure2 – Plot of temperature versus height observed in the wind tunnel at various downwind distances for Condition 3. The figure shows the growth of the TIBL with inland distance

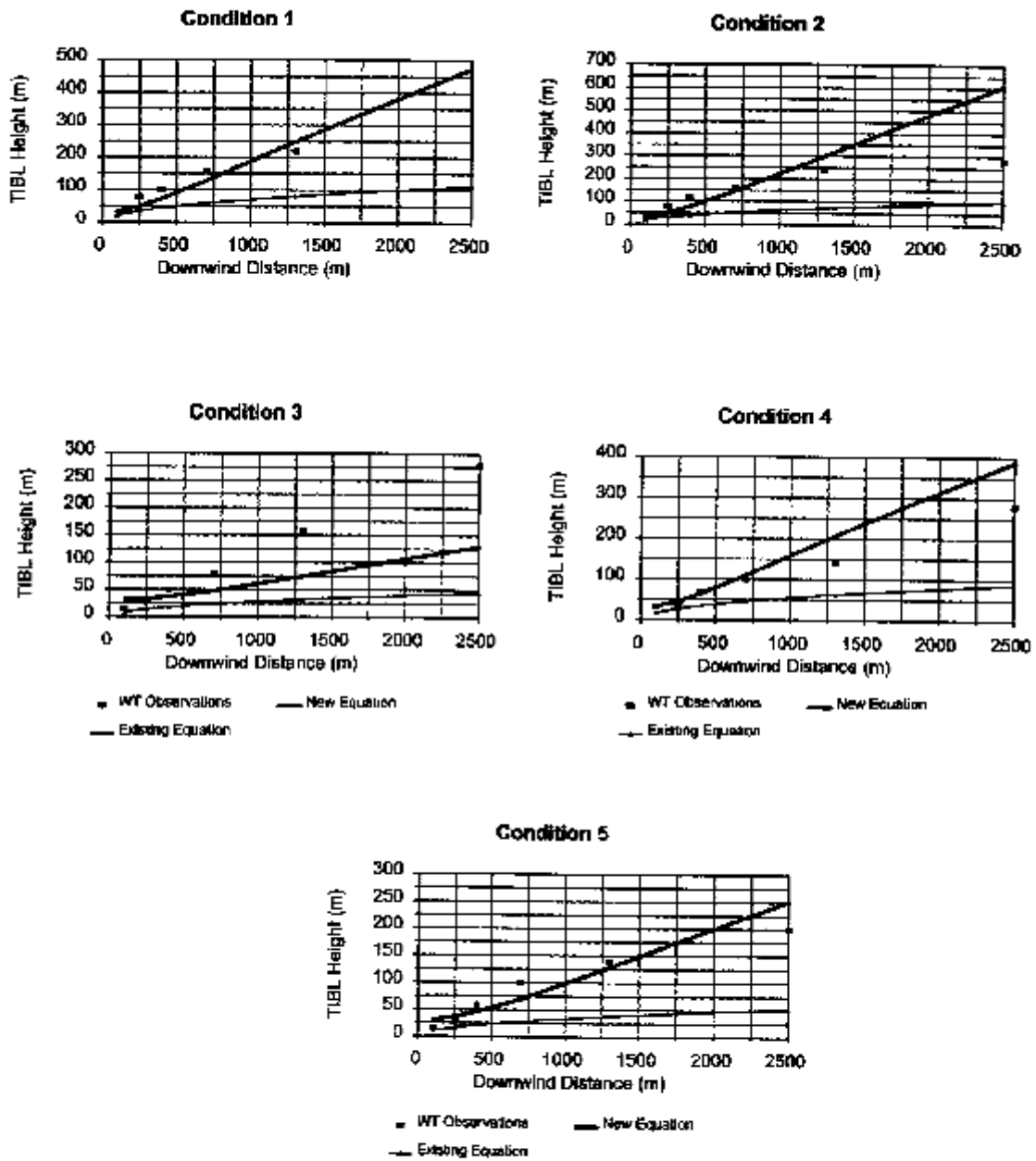


Figure3 - Plot of observed and computed TIBL heights versus inland distance: a) Condition1; b) Condition2; c) Condition 4; d) Condition4; and d) Condition 5

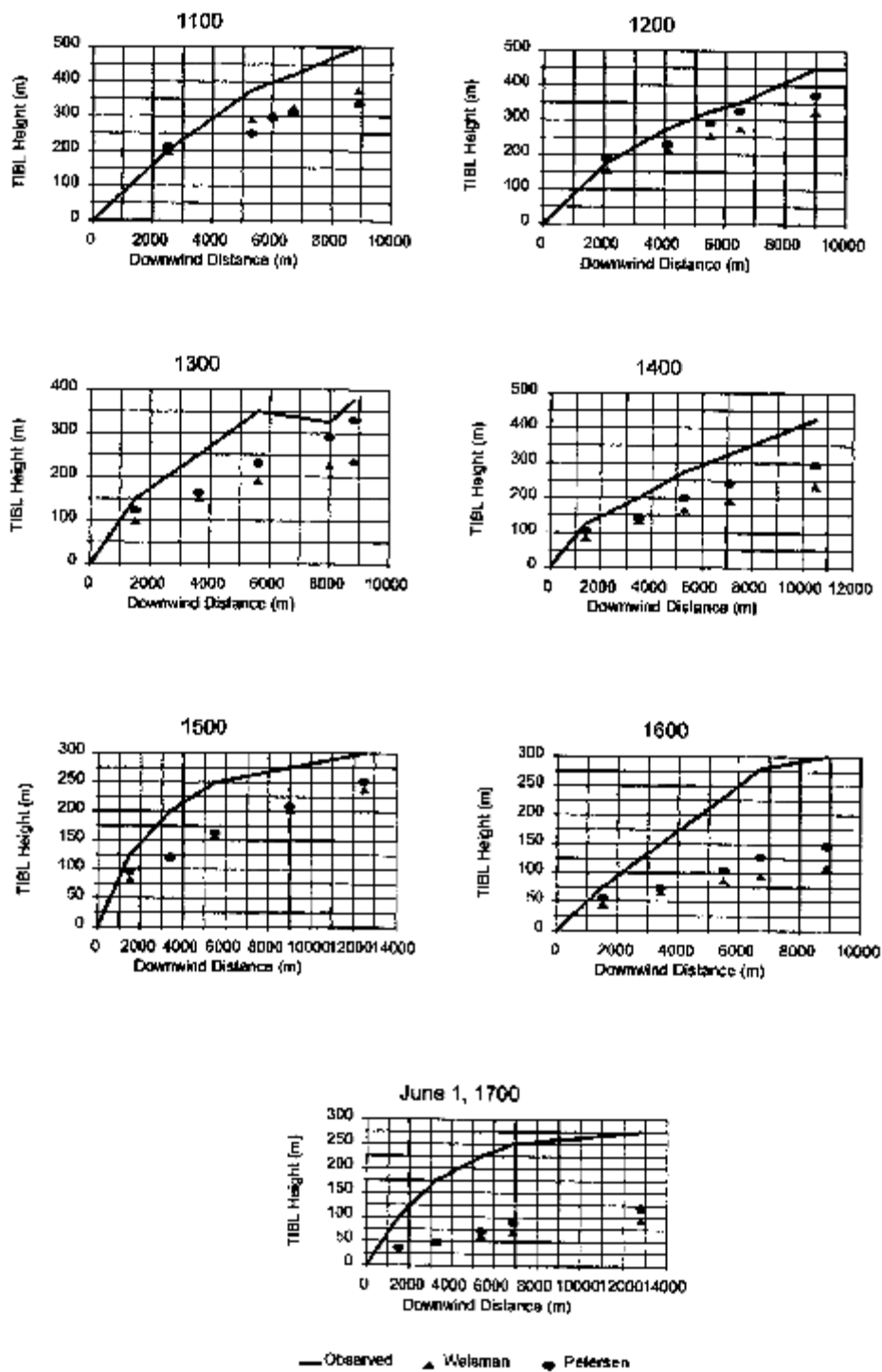


Figure 4 - Plot of observed and computed TIBL heights versus inland distance - June 1 field database.

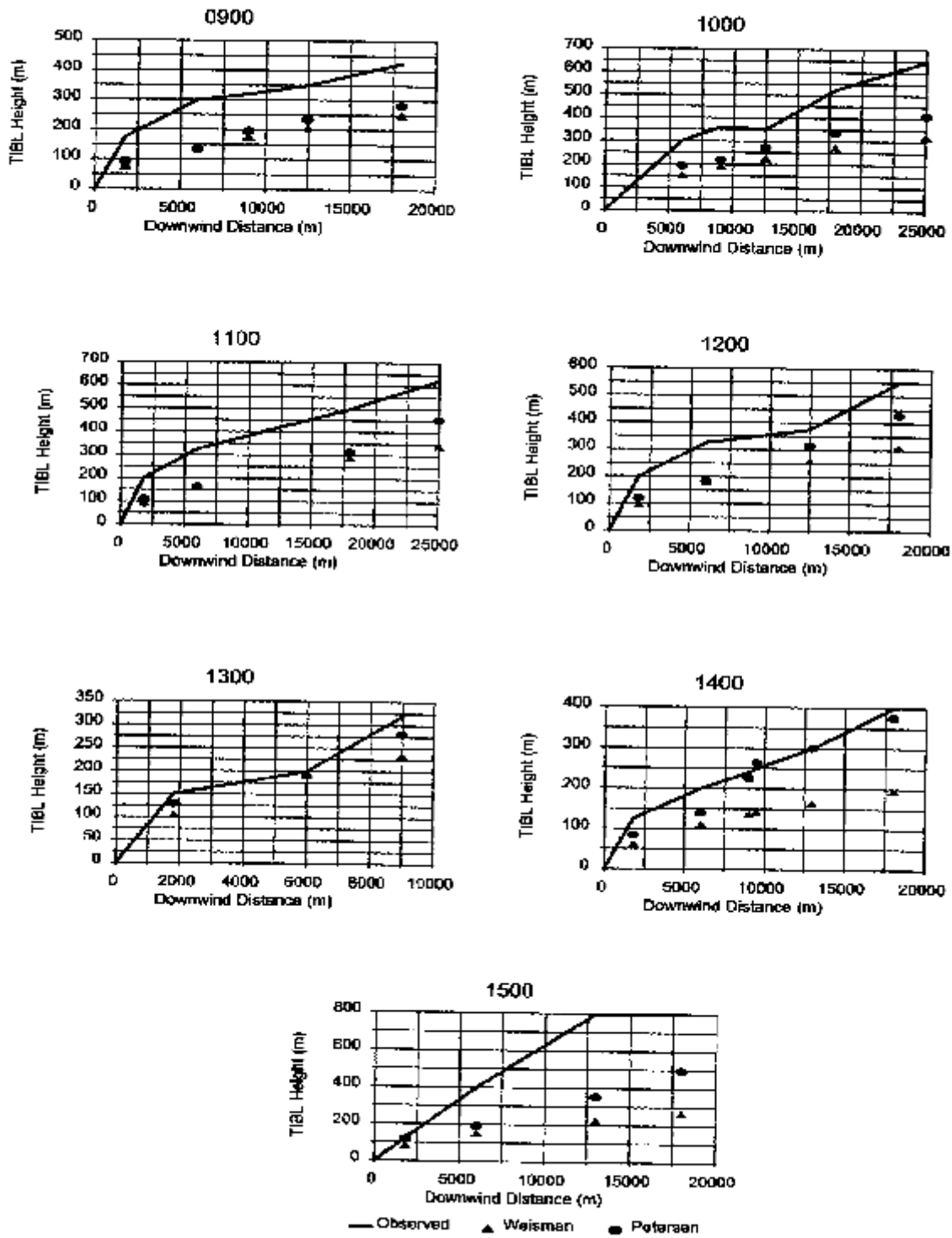


Figure 5 - Plot of observed and computed TIBL heights versus inland distance - June 6 field database.

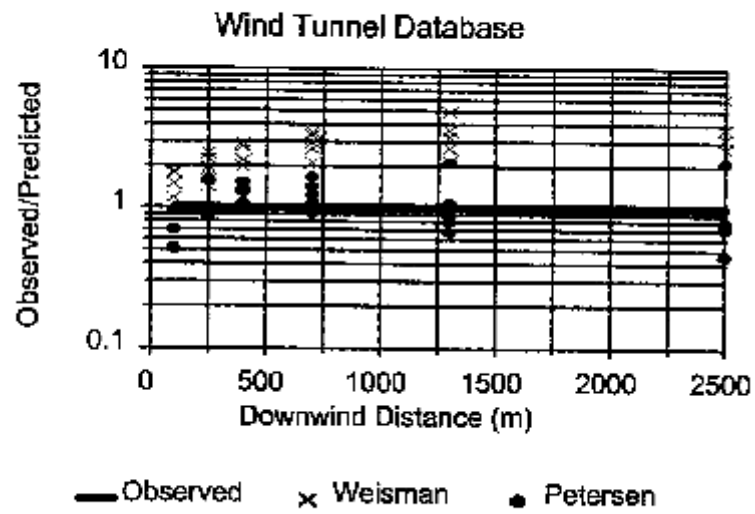


Figure 6a - Ratio of observed to predicted TIBL heights versus downwind distance - wind tunnel database

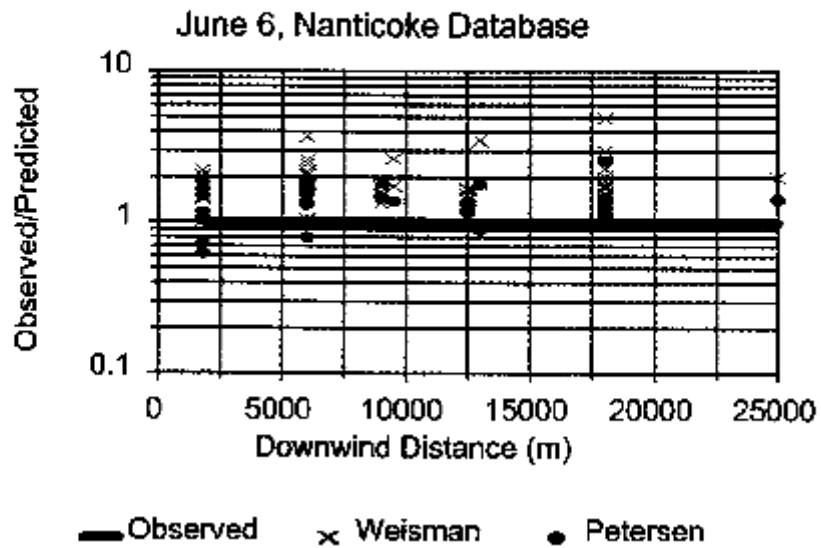
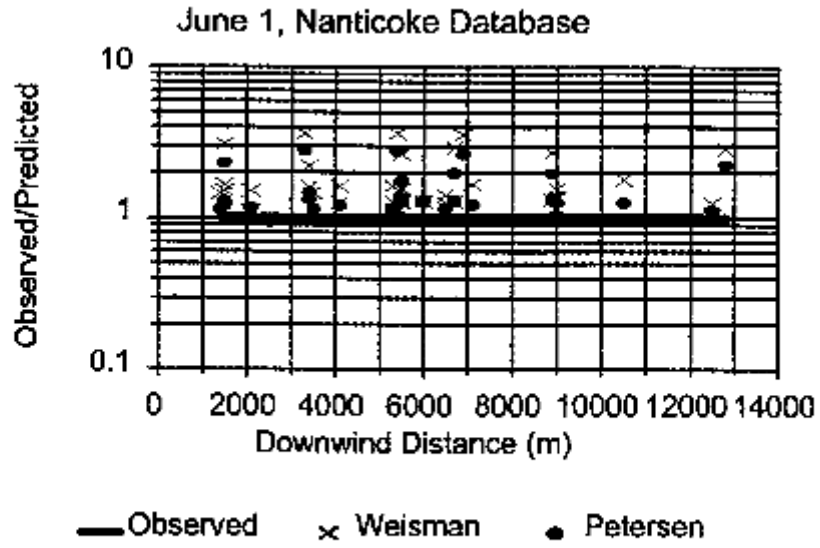


Figure 6 - Ratio of observed to predicted TIBL heights versus downwind distance: b) June 1 field database; c) June 6 field database

WEISMAN - PETERSEN
ALL DATABASES

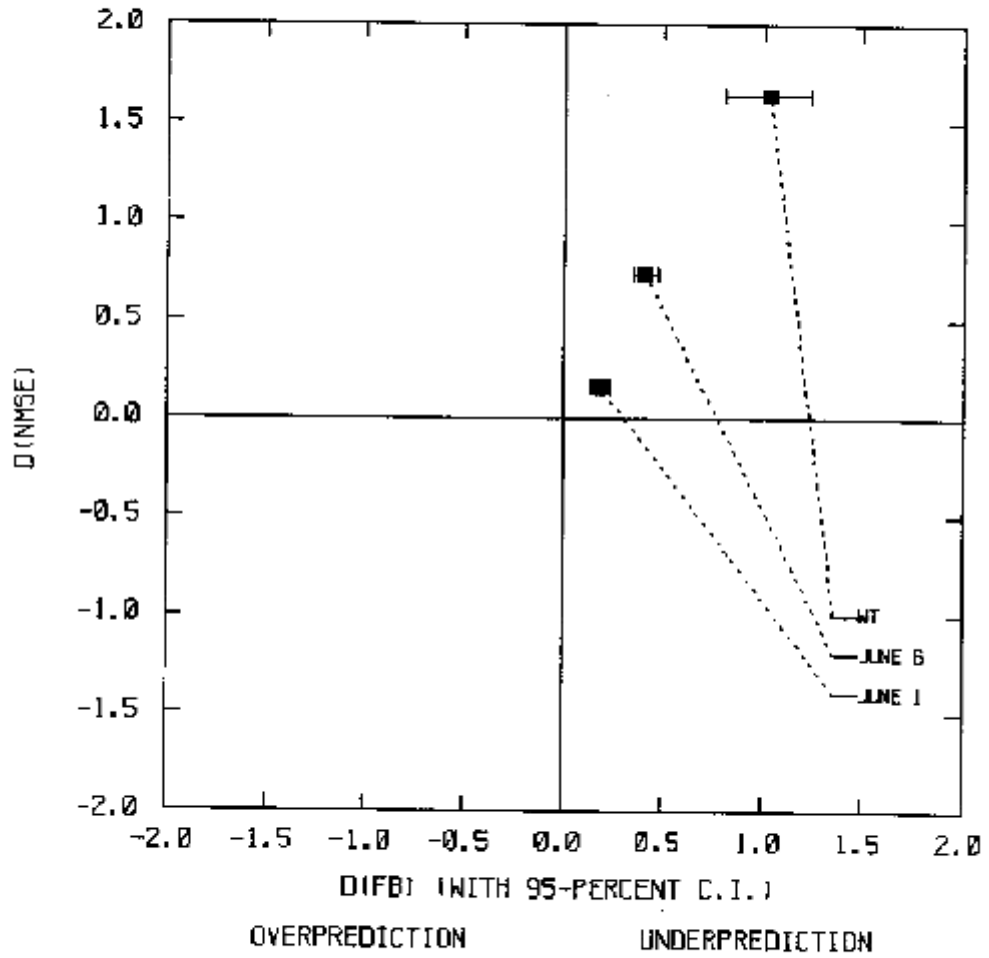


Figure 7 - Differences in NMSE and FB for the two TIBL estimation methods.